Magnetic Trapping of $Co_{core}CoO_{shell}$ Nanoparticles Produced by Gas Phase Reaction

Seung H. Huh[†] and Atsushi Nakajima*[†,††]
[†]*Keio University, Faculty of Science and Technology, Department of Chemistry, 3-14-1 Hiyoshi, Kohoku, Yokohama 223-8522*
[††]*CREST, Japan Science Technology Agency, c/o Department of Chemistry, Keio University, Yokohama, 223-8522*

(Received January 26, 2004; CL-040098)

The magnetic trapping of gas phase $Co_{core}CoO_{shell}$ nanoparticles of ≈160 and 5–10 nm in diameter showed unique patterns of two-dimensional circular or oval distribution and one-dimensional aggregation, respectively, suggesting that granular nanowire can be formed when shell to core ratio is less than ≈0.38 at 0.5 **T**.

Tunneling magnetoresistance (TMR) materials consisting of ferromagnetic layers divided by thin nonmagnetic insulators have been expected to be the state-of-the-art device such as magnetic sensing, or magnetic random access memory because of the controllability of current flow by ferromagnetic spin-direction. In granular Co nanoparticles (NPs) imbedded in insulator matrix film, there is also tunneling current between Co grains that is also controllable by the spin direction of ferromagnetic Co grains.[1–6] However, it has a problem that tunneling current is easily dissipated into the two-dimension, which may cause weak signal for the current detection as the TMR device becomes smaller, or highly integrated to the nanometer-scale.[6,7]

Our goal through this study is the fabrication of one-dimensional (1-D) TMR nanowire expected not only to have the uniaxis flow of the tunneling current along the long-axis but also to obtain the high density. In this letter, it is shown that the magnetic trapping for gas phase $Co_{core}CoO_{shell}$ NP demonstrates the possibility for the producing of 1-D TMR granular nanowire with 5–10 nm in diameter for the first time. Interestingly, moreover, magnetic trapping for the ≈160 nm $Co_{core}CoO_{shell}$ NPs with small ferromagnetic Co cores shows a unique pattern; the dotted line deposition of NPs aggregates with circular or oval distributions of individual NP. This change in the patterns is related to the amounts of the non-ferromagnetic CoO shell.

Details of experimental setup have been described elsewhere.[8] Two kinds of $Co_{core}CoO_{shell}$ NPs with ≈160 nm and 5–10 nm were produced by pulsed laser ablation of a bulk Co metal target; the former was generated in air 300 Torr, and the latter in a mixture of argon 700 and air ≈0.5 Torr. Here O_2 in the air caused CoO because filtering of H_2O by liquid nitrogen trap led to the same result. In these processes, gas phase NPs produced are transported by carrier gas into magnetic field of ≈0.5 **T** applied diagonally in the direction of gravity, and then deposited onto a glass substrate covered with aluminum foil in a magnetic field. The 532 nm photons of Nd^{3+}:YAG laser were used, and typical laser fluence was ≈15 mJ/pulse at a repetition rate of 10 Hz. The flow rate of the carrier gas was 110–130 ml/min. Although it is conceivable to contain non-ferromagnetic CoO or Co_3O_4 NPs in this process, they were excluded from the final products because non-magnetic NPs are not trapped by the confined magnetic field.

Figures 1a and b show scanning electron microscope (SEM) images for the magnetic trapping of the Co/CoO NPs produced in air 300 Torr, and they exhibit unique spots along straight lines, caused by the flow direction of the carrier gas. The magnified images reveal that each spot exhibits circular (Figure 1c), or oval distributions (Figure 1d). The average particle diameter was evaluated as ≈160 nm by fitting a log-normal function (Figure 1f). Figure 2 is the X-ray diffraction (XRD) pattern for the Co/CoO NPs produced in air 300 Torr. Using full-width-at-half-maximum of both Co (111) (0.40°) and CoO (200) facet (0.16°), averaged crystalline size for Co and CoO are estimated to be ≈20 and ≈60 nm, respectively, based on the Scherrer's formula.[9] Together with high-resolution transmission electron microscope (TEM) images, a plausible structure for the Co/CoO NPs is a core Co covered with a CoO shell, because pure Co parts can survive oxidation reaction with the protection of surrounding CoO layer. In fact, the estimated diameter of ≈140 nm (=20 + 60 × 2) is roughly consistent with the average particle diameter of ∼160 nm. The inset of Figure 2 shows the structure of $Co_{core}CoO_{shell}$ NPs from this analysis.

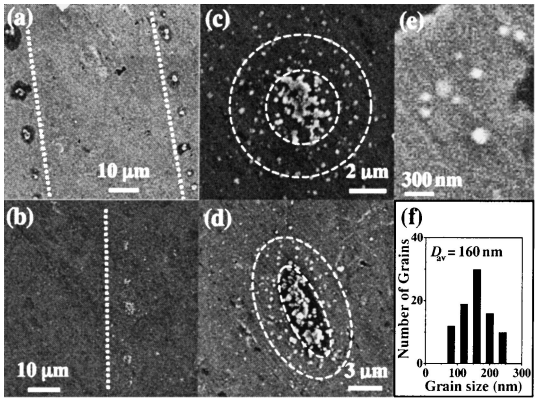

Figure 1. SEM images for Co/CoO nanoparticles having ≈160 nm diameter with magnetic trapping (see text).

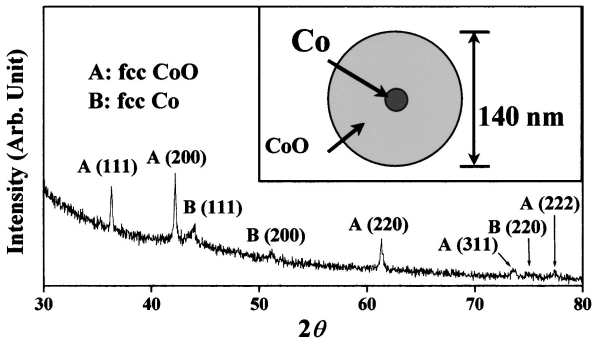

Figure 2. X-ray diffraction for Co/CoO nanoparticles having ≈160 nm diameter, and the inset is their core-shell model.

Copyright © 2004 The Chemical Society of Japan

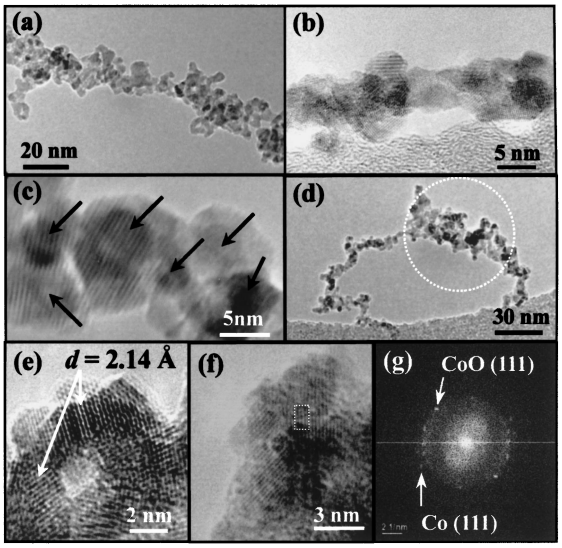

Figure 3. TEM images for 5–10 nm Co/CoO nanoparticles with the magnetic trapping.

Under carrier gas of a mixture of Ar 700 and air ≈0.5 Torr, small $Co_{core}CoO_{shell}$ NPs were produced through the size control[8] in the gas phase reaction. Figure 3 shows TEM images for the magnetic trapping of them. The images clearly show building blocks with core Co and CoO shell: The lattice spacing $d = 2.14$ Å for the shell of Figure 3e indicates the (200) facet of CoO,[10] and the Fourier transform of the lattice fringes of the core-shell NPs of Figure 3f also proves the coexistence of Co (dotted rectangular in Figure 3f) and CoO, as shown in Figure 3g. As indicated by arrows in Figure 3c, moreover, six Co cores are clearly separated by CoO insulator shells, and they tend to align linearly as a nanowire, though their surface morphology is rough and irregular.

As mentioned above, the NP patterns with magnetic trapping exhibit 2-D circular/oval distributions for the ≈160 nm NPs, while they exhibit 1-D aggregations for the ≈10 nm NPs. Since the magnetic trapping force becomes weak for the NPs having thicker CoO shell, this difference can be rationalized by the amounts of non-ferromagnetic CoO shell. The ratio of the CoO shell thickness to the Co core diameter is about 3.0 ($\boldsymbol{R}_1$) for the ≈160 nm NPs, and 0.38 ($\boldsymbol{R}_2$) for the ≈10 nm NPs, where the value of $\boldsymbol{R}_2$ was evaluated as the average for the six particles in Figure 3c. The $\boldsymbol{R}_1/\boldsymbol{R}_2$ ratio is about 7.9, indicating that the interaction with external magnetic field for the NPs with $\boldsymbol{R}_2$ is ≈8 times stronger than that for the NPs with $\boldsymbol{R}_1$.

As reported previously,[8] a linear rod of Co nanoclusters can be generated in carrier gas without oxygen, because a magnetic trapping force is enhanced at its top to increase collision efficiency. The same formation mechanism reasonably leads to linear aggregations of $Co_{core}CoO_{shell}$ NPs as shown in Figure 3. For the NPs having thicker CoO shells, however, it is presumably difficult to make a linear shape because the induced magnetic force of small ferromagnetic cores by external magnetic field is not enough to cancel or compensate the kinetic energy coming from their velocity. There remains a magnetic trapping effect to form the unique circular distribution. That is, the increased magnetic moments as much as $4\pi\mathbf{M}_{group}$ at a group of NPs effectively enhance the external field $\mathbf{H}$ at empty substrate, which results in the total magnetic strength $\mathbf{B}_{group} = \mathbf{H} + 4\pi\mathbf{M}_{group}$.[8] The circular distribution may be provided by a combinatorial result between the $\mathbf{B}_{group}$ strength and kinetic energy distribution of NPs. Namely, the thicker CoO shell results in the morphology change from 1-D to 2-D structures with magnetic trapping. The formation of the oval distribution is rationally considered as the union of two near circular distributions; they grow into one with further deposition due to the enhanced magnetic moments at the overlapped area. It should be noted that the mobility and coalescence of the deposited NPs on the substrate might also contribute the formation of the NPs patterns. Although this mobile coalescence and the direct magnetic trapping are not exclusive each other, the direct magnetic trapping seems dominant considering two facts; (1) center area of the circular distribution exhibits stacking of NPs densely rather than surrounding area, and (2) it seems difficult for the deposited NPs to move around largely because there is somewhat strong magnetic interaction between Co core and external magnet (≈1T at surface).

As shown in the white circle in Figure 3d, furthermore, the coagulated NPs and random aggregated NPs are often observed under TEM observation. The aggregates seemingly come from the NPs with small size ferromagnetic Co cores such the NPs with $\boldsymbol{R}_1$. Although much thinner CoO might form more regular nanowire, this study clearly shows that core to shell ratio ranges from 0 (Co nanocluster)[8] to ≈0.38 for the formation of a magnetic granular nanowire.

We would like to thank the KEIO Center Facilities for Science and Technology Research (CFSTR) for technical support of TEM, SEM, and XRD. This work is partially supported by Grant-in-Aid for 21st century COE program "KEIO LCC" from the Ministry of Education, Culture, Sports, Science, and Technology, Japan.

References

1 V. Skumryev, S. Stoyanov, Y. Zhang, G. Hadjipanayis, D. Givord, and J. Nogués, *Nature*, **423**, 850 (2003).
2 H. Z.-Kolsaraki and H. Micklitz, *Phys. Rev. B*, **67**, 094433 (2003).
3 D. L. Peng, K. Sumiyama, T. Hihara, S. Yamamuro, and T. J. Konno, *Phys. Rev. B*, **61**, 3103 (2000).
4 M. Holdenried, B. Hackenbroich, and H. Micklitz, *J. Magn. Magn. Mater.*, **231**, L13 (2001).
5 H. Fujimori, S. Mitani, and S. Ohnuma, *J. Magn. Magn. Mater.*, **165**, 141 (1997); *J. Magn. Magn. Mater.*, **156**, 311 (1996); *Mater. Sci. Eng., B*, **31**, 219 (1995).
6 K. Yakushiji, S. Mitani, K. Takanashi, S. Takahashi, S. Maekawa, H. Imamura, and H. Fujimori, *Appl. Phys. Lett.*, **78**, 515 (2001).
7 A. E. Mahdi, L. Panina, and D. Mapps, *Sens. Actuators, A*, **105**, 271 (2003).
8 S. H. Huh, A. Nakajima, and K. Kaya, *J. Appl. Phys.*, **95**, 2732 (2004).
9 B. D. Cullity, "Elements of X-ray Diffraction," Addison-Wesley (1978), p 139.
10 "Powder Diffraction File," ed. by L. G. Berry, Joint Committee on Powder Diffraction Standards, Pennsylvania (1972), Inorganic Volume, Set 48, p 673, Card No. 48-1719.

Published on the web (Advance View) March 15, 2004; DOI 10.1246/cl.2004.428